International Journal of Steel Structures 17(2): 491-499 (2017)
DOI 10.1007/s13296-017-6009-5
ISSN 1598-2351 (Print)
ISSN 2093-6311 (Online)

International Journal of
STEEL
STRUCTURES
www.springer.com/journal/13296

Nonlinear Bending of Box Section Beams of Finite Length Under Uniformly Distributed Loading

Wei-bin Yuan[1,2,*], Zhao-shui Bao[1], Nan-ting Yu[1], Shuang-shuang Zhu[1], and Li-ping Wu[3]

[1]*College of Civil Engineering and Architecture, Zhejiang University of Technology, Hangzhou, 310014, Zhejiang China*
[2]*Key Laboratory of Civil Engineering Structures & Disaster Prevention and Mitigation, Technology of Zhejiang Province, Hangzhou, 310014, Zhejiang China*
[3]*Hangzhou Polytechnic, Hangzhou, 311402, Zhejiang China*

Abstract

In this paper, the bending response of box-section beams of finite length is investigated by using energy methods. The basic assumptions used in the present study are that the total strain energy of a box-section beam subjected to uniformly distributed loading can be simplified into a two-stage analysis process. One is the local bending response of the webs and flanges behaving as plates; the other is the overall bending response of the beam with a deformed cross-section. Analytical solutions for both static and dynamic instabilities of box section beams of finite length subjected to transverse uniformly distributed loading are derived by applying the minimum potential energy principle. To validate the analytical solutions developed, geometric nonlinear finite element analyses are also conducted. Good agreement between the present solutions and the FEA results is demonstrated. Finally, the effects of beam length on the limit critical uniformly distributed load are also discussed.

Keywords: uniformly distributed loading, nonlinear instability, box-section beam, flattening

1. Introduction

Cold-formed thin-walled box section beams have been increasingly used as structural components in building and many other civil engineering fields. When a thin-walled box section beam is subjected to a bending load, Brazier type flattening deformation would occur in the section, which can lead the beam to have a nonlinear bending response and snap through instability.

The literature survey shows that, most of existing studies on thin-walled box section members focused on the buckling or curling of the members when they are subjected to axial and/or bending loads. For example, Lanc *et al.* (2015) applied the Euler-Bernoulli beam theory for bending and the Vlasov theory for torsion to investigate the buckling problem of thin-walled functionally graded sandwich box beams. Bedair (2015) presented a new analytical expression for computing web shear buckling of box sections by taking account for flange restraints. The expression was validated by the results obtained using semi-analytical finite strip method. Li and Luo (2015) investigated the seismic behavior and relevant buckling mechanisms of eccentrically compressed steel box columns. Shen (2015) developed a double nonlinear finite element model that can take account of both geometric and material imperfections to analyze ultimate carrying capacity of eccentrically loaded welded thin-webbed rectangular section columns. The interaction between local and overall buckling of welded stainless steel columns has been investigated experimentally and numerically by Yuan *et al.* (2015). Vanegas and Patino (2013) applied the updated Lagrangian formulation for non-linear finite element analysis to the problem of thin-walled composites box beams undergoing large displacements. Jang *et al.* (2013) presented a higher-order beam analysis which was applied to three thin-walled box beams connected at a joint under out-of-plane bending loads. Vo and Lee (2010) investigated numerically the effects of axial force, bending moment, fiber orientation on the buckling loads, buckling moments, natural frequencies and corresponding vibration mode shapes as well as the axial-moment-frequency interaction curves about thin-walled composite box beams, from which they presented (Vo and Lee, 2009) a general geometrically nonlinear model for thin-walled composite space beams with arbitrary lay-ups under various types of loadings. Kim (2009) presented the exact solutions for the spatially coupled free vibration analysis of composite box beams resting on

Received January 27, 2016; accepted October 18, 2016;
published online June 30, 2017

*Corresponding author
Tel: +86-517-88320277, Fax: +86-571-88320460
E-mail: yuanwb@zjut.edu.cn

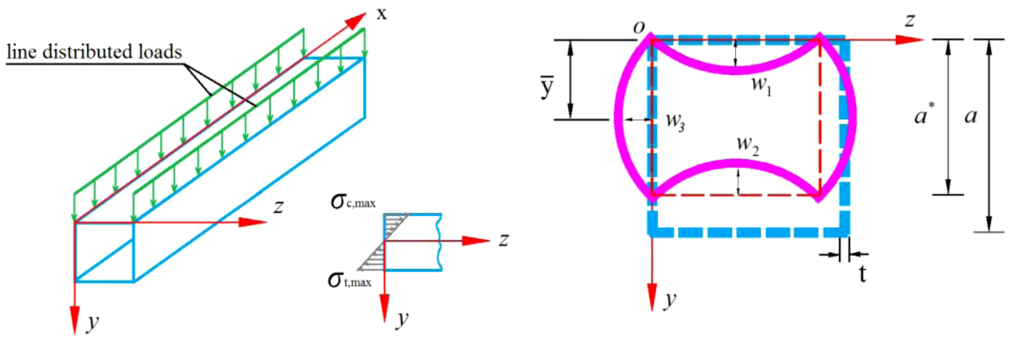

(a) Geometry of box-section beam (b) Definition of symbols and notations

Figure 1. (a) Geometry of box-section beam. (b) Definition of symbols and notations.

elastic foundation under axial loading. Hwang *et al.* (2009) presented the experimental results on the strength behavior and failure modes of box beam-to-circular column connections in steel piers. Liu provided an optimum design of cross-sectional profiles for regular thin-walled box section beams (Liu, 2009) and proposed simplified analysis models for thin-walled box section beams through crashworthiness analyses (Liu *et al.*, 2009). Wu *et al.* (2003) presented an initial value solution of the static equilibrium differential equations of thin-walled box beams, considering both shear lag and shear deformation. Kim *et al.* (2003) carried out a higher-order one-dimensional analysis of the in-plane flexural deformation of thin-walled curved box beams and demonstrated the significant contribution of the bending distortion to the beam flexibility. Kotelko *et al.* (2000) presented the experimental results of the post-failure behaviour of box section beams subjected to pure bending. Note that when a box-section beam is bent about its neutral axis, Brazier type of flattening deformation would occur in the section, which can lead the beam to have a nonlinear bending response and a snap-through instability (Brazier, 1927). However, despite the large number of publications on thin-walled steel box section members, there is little work found on the nonlinear analysis with considering the effect of cross-sectional deformation on the overall bending response of the member. In this paper, a modified Brazier approach is used to investigate the nonlinear bending response of thin-walled box section beams of finite length. The basic assumptions used in this study are that the deformation of the beam subjected to a uniformly distributed load can be simplified into a two-stage analysis process. One is the local bending response of the webs and flanges behaving as the plate; the other is the overall bending response of the beam with a flattened cross-section. The nonlinear bending response is analyzed by using the minimum potential energy principle from which a critical load associated with section flattening-induced buckling is determined analytically.

2. Physical Model and Formulations

Consider a thin-walled box section beam subjected to a uniformly distributed load acting on the top web. For the simplicity of analysis, the uniformly distributed load is simplified as two line distributed loads acting on the intersection lines between the top flange and two side webs, in which the bending is about beam neutral axis so that the top flange is in compression and bottom flange is in tension (Fig. 1(a)). The boundary conditions of the beam are assumed to be simply supported in both ends. With the increase of the load, the cross-section will be flattened as shown in Fig. 1(b) due to the Brazier effect. Thus the deformations of the box section beam can be characterized by the overall bending deformation of the beam (beam-type bending) and the local distortional deformation of the beam cross-section (section flattening). For a beam of finite length, the flattening of the beam cross-section will be not uniform because of the effect of boundaries. The following displacements can be assumed for the box section beam of finite length, subjected to a static uniformly distributed load.

$$v(x) = A\sin\left(\frac{\pi x}{l}\right) \tag{1}$$

$$w_1(x,z) = w_{1\max}\sin\left(\frac{\pi z}{a}\right)\sin\left(\frac{\pi x}{l}\right) \tag{2}$$

$$w_2(x,z) = -w_{2\max}\sin\left(\frac{\pi z}{a}\right)\sin\left(\frac{\pi x}{l}\right) \tag{3}$$

$$w_3(x,y) = \frac{-\pi(a-y)y(w_{1\max}a - w_{1\max}y + w_{2\max}y)}{a^3}\sin\left(\frac{\pi x}{l}\right) \tag{4}$$

where $v(x)$ is the overall bending deflection of the beam, $w_1(x,z)$ is the local displacement of the top flange, $w_2(x,z)$ is the local displacement of the bottom flange, $w_3(x,y)$ is

the local displacement of the side webs, A is the constant to be determined, $w_{1\max}$ is the maximum deflection of top flange (relative to its two edges), $w_{2\max}$ is the maximum deflection of bottom flange (relative to its two edges), z and y are the local coordinates as shown in Fig. 1(b), a is the width of flanges/webs, and l is the beam length. The local bending strain energy, U_1, of the flanges and webs generated due to the flattening displacements $w_1(x,z)$, $w_2(x,z)$ and $w_3(x,y)$ can be expressed as follows,

$$\begin{aligned} U_1 &= \frac{D}{2}\int_0^l\int_0^a \left\{\left(\frac{\partial^2 w_1}{\partial z^2}+\frac{\partial^2 w_1}{\partial x^2}\right)^2 - 2(1-v)\left[\frac{\partial^2 w_1}{\partial z^2}\frac{\partial^2 w_1}{\partial x^2}-\left(\frac{\partial^2 w_1}{\partial z\partial x}\right)^2\right]\right\} dz dx \\ &+ \frac{D}{2}\int_0^l\int_0^a \left\{\left(\frac{\partial^2 w_2}{\partial z^2}+\frac{\partial^2 w_2}{\partial x^2}\right)^2 - 2(1-v)\left[\frac{\partial^2 w_2}{\partial z^2}\frac{\partial^2 w_2}{\partial x^2}-\left(\frac{\partial^2 w_2}{\partial z\partial x}\right)^2\right]\right\} dy dx \\ &+ D\int_0^l\int_0^a \left\{\left(\frac{\partial^2 w_3}{\partial y^2}+\frac{\partial^2 w_3}{\partial x^2}\right)^2 - 2(1-v)\left[\frac{\partial^2 w_3}{\partial y^2}\frac{\partial^2 w_3}{\partial x^2}-\left(\frac{\partial^2 w_3}{\partial y\partial x}\right)^2\right]\right\} dy dx \end{aligned} \tag{5}$$

where $D = \dfrac{Et^3}{12(1-v^2)}$ is the flexural rigidity of the plate (flanges and webs), E is the Young's modulus, n is the Poisson's ratio, t is the thickness of the plate (flanges and webs). Substituting Eqs. (2), (3) and (4) into (5), it yields,

$$\begin{aligned} U_1 &= \frac{D\pi^2}{420a^3l^3}\begin{pmatrix} 840l^4w_{2\max}^2 + 56a^2l^2\pi^2w_{2\max}^2 + 2a^4\pi^4w_{2\max}^2 - 840l^4w_{1\max}w_{2\max} \\ +28a^2l^2\pi^2w_{1\max}w_{2\max} + 3a^4\pi^4w_{1\max}w_{2\max} + 840l^4w_{1\max}^2 \\ +56a^2l^2\pi^2w_{1\max}^2 + 2a^4\pi^4w_{1\max}^2 \end{pmatrix} \\ &+ \frac{D(a^4+2a^2l^2+l^4)\pi^4w_{1\max}^2}{8a^3l^3} + \frac{D(a^4+2a^2l^2+l^4)\pi^4w_{2\max}^2}{8a^3l^3} \end{aligned} \tag{6}$$

The overall bending strain energy, U_2, of the beam with a flattened cross-section can be expressed in terms of the bending strain energy of the beam as follows,

$$U_2 = \frac{1}{2}\int_0^l EI_w^*\left(\frac{d^2v}{dx^2}\right)dx \tag{7}$$

where I_w^* is the second moment of area of the distorted beam cross-section by taking into account the effect of distortion and translation of sectional elements, which can be expressed as follows,

$$I_w^* = \left(\frac{a^*}{a}\right)^2 I_w \tag{8}$$

where I_w is the second moment of area of the cross-section only taking into the effect of distortion, a^* is the vertical distance from top flange edge to the bottom flange edge taking into account the effect of translation of sectional elements (Fig. 1(b)), which can be expressed as follows,

$$I_w = t\left(\int_0^a (w_1-\bar{y})^2dz + \int_0^a (\bar{y}-w_2)^2dz + 2\int_0^a (y-\bar{y})^2dy\right) \tag{9}$$

$$a^* = \int_0^a \left[1-\frac{1}{2}\left(\frac{dw_3}{dx}\right)^2\right]dy \tag{10}$$

where $\bar{y}$ is the vertical distance from the neutral axis to the intersection point of the top flange and side web (Fig. 1(b)), which can be expressed as follows,

$$\bar{y} = \frac{1}{4a}\left(\int_0^a w_1dz + 2\int_0^a ydy + \int_0^a w_2dz\right) \tag{11}$$

Substituting Eqs. (2) and (3) into (9) and (11), and ignoring the terms of higher order $w_{1\max}$ and $w_{2\max}$, it yields,

$$I_w = \frac{ta^3}{6} + \frac{a^2t\left(a\pi - 4w_{2\max}\sin\left(\frac{\pi x}{l}\right) - 4w_{1\max}\sin\left(\frac{\pi x}{l}\right)\right)}{2\pi} \tag{12}$$

$$\bar{y} = \frac{a\pi - w_{2\max}\sin\left(\frac{\pi x}{l}\right) + w_{1\max}\sin\left(\frac{\pi x}{l}\right)}{2\pi} \tag{13}$$

Substituting Eq. (4) into (10), it yields,

$$a^* = -\frac{-30a^2 + 2\pi^2 w_{2\max}^2 \sin^2\left(\frac{\pi x}{l}\right) + \pi^2 w_{1\max} w_{2\max} \sin^2\left(\frac{\pi x}{l}\right) + 2\pi^2 w_{1\max}^2 \sin^2\left(\frac{\pi x}{l}\right)}{30a} \tag{14}$$

Substituting Eqs. (9) and (14) into (8), it yields,

$$I_w^* = -\frac{1}{1350a^2\pi} t\left(-a\pi + 3w_{2\max}\sin\left(\frac{\pi x}{l}\right) + 3w_{1\max}\sin\left(\frac{\pi x}{l}\right)\right) \left(-30a^2 + 2\pi^2 w_{2\max}^2 \sin^2\left(\frac{\pi x}{l}\right) + \pi^2 w_{1\max} w_{2\max} \sin^2\left(\frac{\pi x}{l}\right) + 2\pi^2 w_{1\max}^2 \sin^2\left(\frac{\pi x}{l}\right)\right)^2 \tag{15}$$

Substituting Eqs. (1) and (15) into (7), it yields,

$$U_2 = \frac{\left(\begin{array}{l} 252000a^5\pi^2 - 2016000a^4(w_{1\max} + w_{2\max}) - 12600a^3\pi^4 \\ (2w_{2\max}^2 + 2w_{1\max}^2 + w_{1\max}w_{2\max}) + 175a\pi^6 \\ A^2 E\pi^2 t \left(2w_{2\max}^2 + 2w_{1\max}^2 + w_{1\max}w_{2\max}\right)^2 - 1536\pi^4(w_{1\max} + w_{2\max}) \\ (2w_{2\max}^2 + 2w_{1\max}^2 + w_{1\max}w_{2\max})^2 + 107520a^2\pi^2 \\ (2w_{2\max}^3 + 3w_{2\max}^2 w_{1\max} + 3w_{1\max}^2 w_{2\max} + 2w_{1\max}^3) \end{array}\right)}{1512000a^2 l^3} \tag{16}$$

The potential of the uniformly distributed load can be calculated as follows,

$$W = \int_0^l q v(x) dx = \frac{2qlA}{\pi} \tag{17}$$

where q is the density of the uniformly distributed load. The total potential of the system thus is expressed by:

$$\Pi = U_1 + U_2 - W \tag{18}$$

3. Nonlinear Bending Response in Static Analysis

The flattening-induced nonlinear bending response of thin-walled box section beams under uniformly distributed loading can be obtained either by solving the nonlinear bending equations of flange and web plates or by using the energy method. Experience showed that it is more convenient to use the energy method (Brazier, 1927). Using the principle of minimum potential energy the following equilibrium equations can be obtained,

$$\frac{\partial \Pi(A, w_{1\max}, w_{2\max}, q)}{\partial w_{1\max}} = f_1(A, w_{1\max}, w_{2\max}) = 0 \tag{19}$$

$$\frac{\partial \Pi(A, w_{1\max}, w_{2\max}, q)}{\partial w_{2\max}} = f_2(A, w_{1\max}, w_{2\max}) = 0 \tag{20}$$

$$\frac{\partial \Pi(A, w_{1\max}, w_{2\max}, q)}{\partial A} = f_3(A, w_{1\max}, w_{2\max}, q) = 0 \tag{21}$$

For a given loading density q, one can determine the constant A and the flattening displacements $w_{1\max}$ and $w_{1\max}$ by solving Eqs. (19), (20) and (21). It is obvious that Eqs. (19), (20) and (21) are nonlinear, which means that A, $w_{1\max}$ and $w_{2\max}$ increase with the loading density but do not follow the simple linear relationship as provided in the linear bending theory of beams. In order to solve the set of nonlinear equations, the Newtonian iteration method has been chosen. Note that for most cases the flattening displacements $w_1(x,z)$, $w_2(x,z)$ and $w_3(x,y)$ of the beam cross-section would be much small compared to the overall bending deflection of the beam $v(x)$ due to the fact that for the beam subjected to uniformly distributed loading the dominant deformation is still the bending deformation. This means that all nonlinear terms in Eq. (21) would be smaller than the linear term in terms of the order of magnitude. By neglecting the nonlinear terms related to A, $w_{1\max}$ and $w_{2\max}$, Eq.(21) can be simplified as:

$$\frac{a^3 AE\pi^4 t}{3l^3} - \frac{2lq}{\pi} = 0 \tag{22}$$

From Eq. (22) A ($=A_0$) can be solved for a given q. Afterwards, by neglecting the nonlinear terms related to $w_{1\max}$ and $w_{2\max}$ in Eqs. (19) and (20), $w_{1\max}$ and $w_{2\max}$ can be calculated using Eqs. (19) and (20) by using $A = A_0$. Replace the nonlinear terms related to $w_{1\max}$ and $w_{2\max}$ in Eqs. (19) and (20) with newly obtained $w_{1\max}$ and $w_{2\max}$. Then, use new Eqs. (19) and (20) to recalculate $w_{1\max}$ and $w_{2\max}$. An iteration is further used in which new $w_{1\max}$ and $w_{2\max}$ are recalculated again from new Eqs. (19) and (20) in which the nonlinear terms related to $w_{1\max}$ and $w_{2\max}$

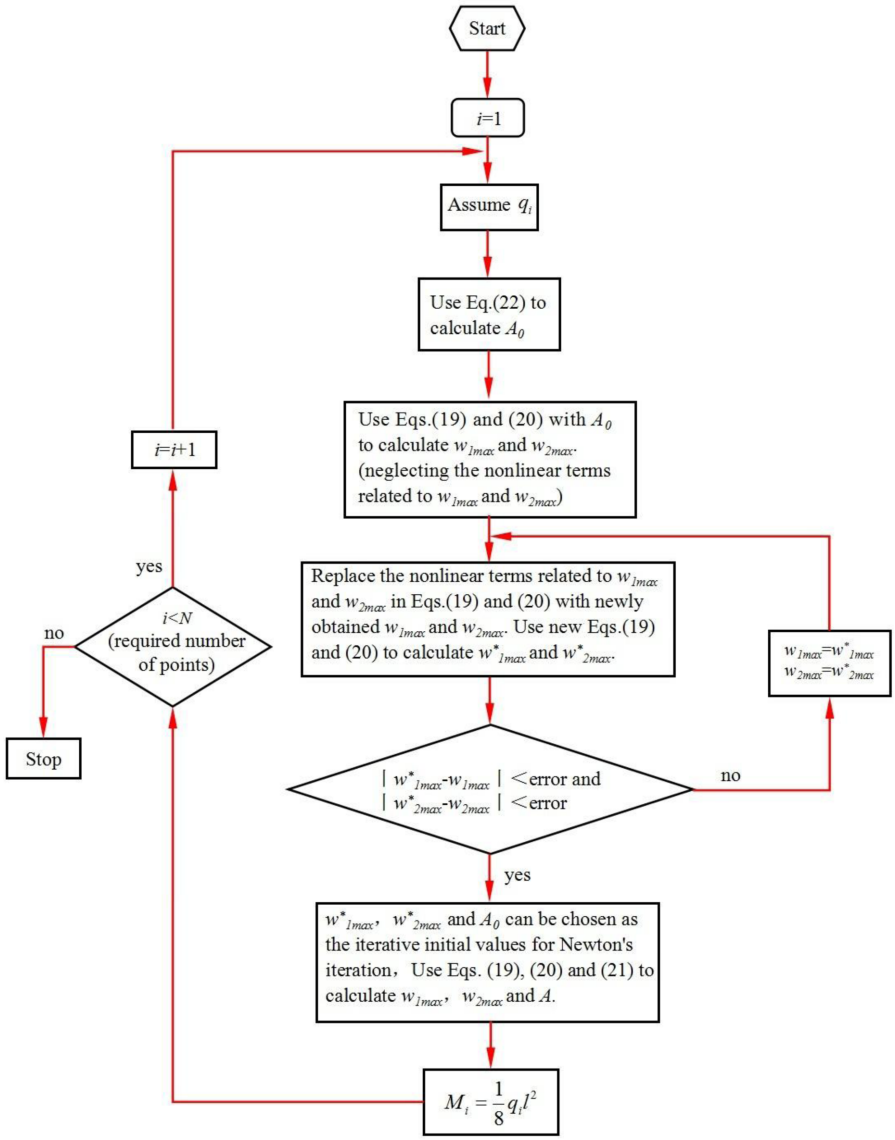

Figure 2. Flowchart for calculation.

are replaced by using newly obtained w_{1max} and w_{2max}. This routine is repeated until the solution converges. A detailed iterative process is provided in Fig. 2.

In order to validate the analytical solution shown above, finite element analyses considering geometric nonlinearity have been performed using ANSYS, in which the box-section beam analyzed is a =80 mm, t =1.5 mm, with beam lengths from l =1500 mm to l =2000 mm and elastic material properties, E =206 GPa and n =0.3. In the finite element analysis, only a half of the beam was modelled because of symmetry. A general type of four-node shell element (shell 143) was used. The boundary conditions are defined as follows. At one end of the beam, the four corners of the beam cross-section are assumed to have zero displacements in both vertical (y) and lateral (z) directions, whereas at the other end (mid-section of the beam) a symmetrical boundary condition is enforced. In the finite element analysis the uniformly distributed load is applied on the intersection lines between the top flange and side webs (Fig. 3).

Figures 4-5 show the comparisons of the moment-displacement curves between the present solutions and the finite element analysis results for two different beam lengths, where the moment is calculated based on the loading density and beam length, that is $M=ql^2/8$, and the overall deflection of the beam, d, is at the top of the web on the symmetric section (that is the mid-section of the beam). It can be seen from the figures that, the present prediction of the maximum moment agrees very well with that obtained from the nonlinear finite element analysis although the corresponding displacement predicted at the peak point is slightly smaller than that shown in the finite element analysis. Also, it can be seen from Figs. 4 and 5 that the agreement of the prediction with the finite element

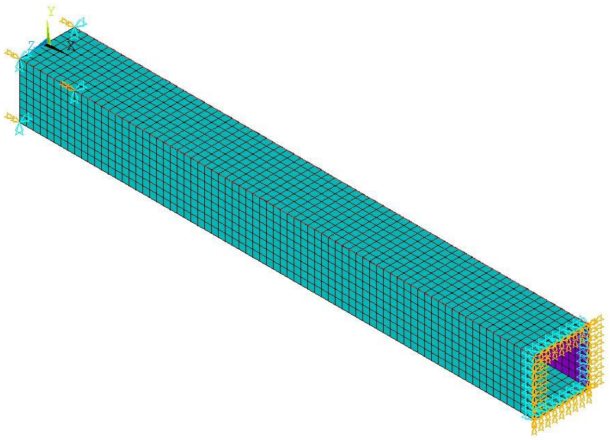

Figure 3. Finite element analysis model and element mesh (half length of the beam).

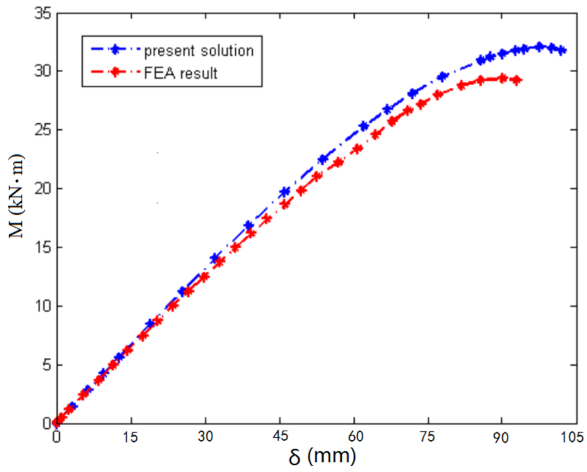

Figure 4. Comparison of moment-deflection curves between present and finite element analyses (a=80 mm, t=1.5 mm, l=1500 mm, E=206 GPa, n=0.3).

solution is very good when the load/deflection is small. Divergence of the two solutions is observed when the load is near to the limit critical load. This is probably because only linear terms in the strain-displacement equations are used in the analytical solution. Since the finite element method employed uses the geometric nonlinear shell elements the analysis includes not only the section fattening but also others such as the deflection-induced membrane action and the secondary warping through the plate thickness direction. These effects are not considered in the present analytical model. Nevertheless, the results shown in Figs. 4 and 5 demonstrate that the section flattening has the dominant effect on the bending behavior of box section beams and can cause the beam to have snap-through instability.

Figure 6 shows the comparison of moment-deflection curves of the beams with various different lengths. It can be seen from the figure that the maximum moment decreases slightly with the increase of the beam length. However,

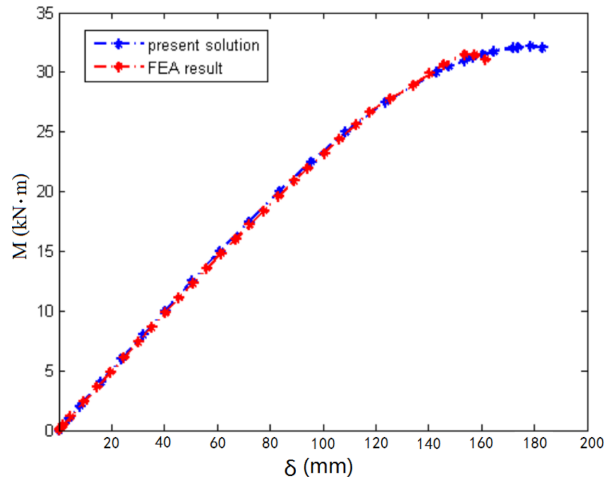

Figure 5. Comparison of moment-deflection curves between present and finite element analyses (a=80 mm, t=1.5 mm, l=2000 mm, E=206 GPa, n=0.3).

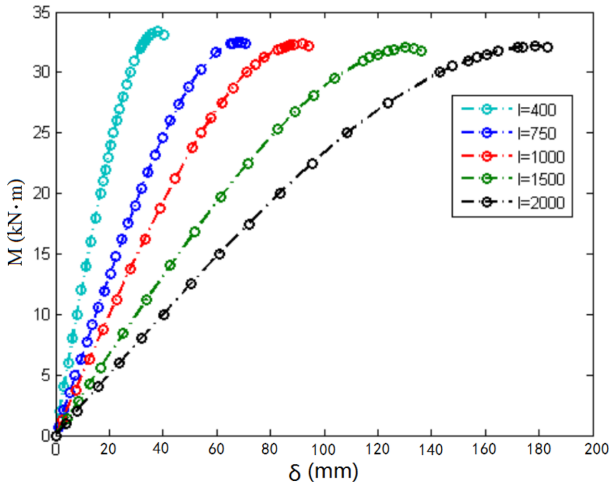

Figure 6. Moment-deflection curves for beams with different beam lengths (a=80 mm, t=1.5 mm, E=206 GP, n=0.3).

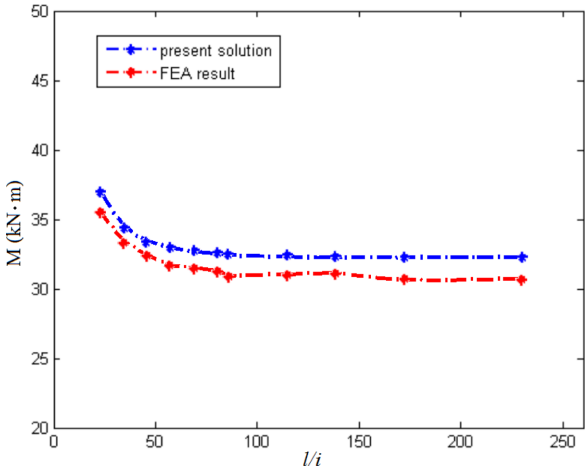

Figure 7. Critical moment versus slenderness ratio (a=110 mm, t=1.5 mm, E=206 GP, n=0.3).

the maximum deflection at the peak point increases rather quickly with the increase of the beam length. The nonlinearity of the moment-deflection curve also increases with increased beam length.

Figure 7 shows the variation of the limit critical moment (that is the moment at peak point) with the beam length. As to be expected, the limit critical moment decreases with the increase of the beam length. It is worth noting that, for small ratio of l/i, where i is the gyration radius, the curve is remarkably steep due to the effect of boundary restraints on the displacements. For large ratio of l/i, however, the curve tends to the analytical solution of infinite length. The reason for this is probably due to the sine-series displacement functions employed in the present approach, which has a localized effect near boundaries even for the beam of infinite length.

4. Nonlinear Bending Response in Dynamic Analysis

It is well known that the dynamic instability characteristics of structures subjected to sudden step loads (that is the dynamic step-loads) are similar to their static instability characteristics although the critical dynamic loads are often smaller than the corresponding critical static loads (Li *et al.*, 1997; Li, 1996). By using similar kinematic assumptions employed in the static analysis the critical dynamic instability loads can be determined based on the energy principle (Li *et al.*, 1997; Li, 1996). For the case where the box-section beam is subjected to a sudden step distributed load $q^*(t)$ where $q^*(t)=0$ at $t=0$ and $q^*(t)=q$ for $t>0$ (q is a constant), the equation of motion of the beam can be written in the form of energy conservation,

$$T\left(\frac{dA}{dt}, \frac{dw_{1\max}}{dt}, \frac{dw_{2\max}}{dt}\right) + \Pi(A, w_{1\max}, w_{2\max}, q) = 0 \quad (23)$$

where T is the total kinetic energy and P is the total potential energy defined in Eq. (18). The zero set on the right-hand side of the equation is because the total potential energy is defined in such a way that it is zero at the initial time ($A=w_{1\max}=w_{2\max}=0$).

Physically, Eq. (23) defines the time responses of A, $w_{1\max}$ and $w_{1\max}$ for a given q. In order to determine the critical dynamic load q and corresponding critical dynamic moment, it is assumed that when the bending deflection response reaches its extreme value, the flattening deformation response also reaches its extreme value (Li *et al.*, 1997; Li, 1996). According to this assumption, since the rates, dA/dt, $dw_{1\max}/dt$, $dw_{2\max}/dt$, are equal to zero when the responses reach their extreme values, the maximum amplitudes of A, $w_{1\max}$ and $w_{1\max}$ can be determined by letting $dA/dt=dw_{1\max}/dt=dw_{2\max}/dt=0$ in Eq. (23), that is,

$$\Pi(A, w_{1\max}, w_{2\max}, q) = 0 \quad (24)$$

Differentiation of Eq. (24) with respect to A, $w_{1\max}$ and $w_{2\max}$, it yields,

$$\frac{\partial \Pi(A, w_{1\max}, w_{2\max}, q)}{\partial A} + \frac{\partial \Pi(A, w_{1\max}, w_{2\max}, q)}{\partial q}\frac{\partial q}{\partial A} = 0 \quad (25)$$

$$\frac{\partial \Pi(A, w_{1\max}, w_{2\max}, q)}{\partial w_{1\max}} + \frac{\partial \Pi(A, w_{1\max}, w_{2\max}, q)}{\partial q}\frac{\partial q}{\partial w_{1\max}} = 0 \quad (26)$$

$$\frac{\partial \Pi(A, w_{1\max}, w_{2\max}, q)}{\partial w_{2\max}} + \frac{\partial \Pi(A, w_{1\max}, w_{2\max}, q)}{\partial q}\frac{\partial q}{\partial w_{2\max}} = 0 \quad (27)$$

Note that when the dynamic instability occurs, $M/A = M/w_{1\max} = M/w_{2\max} = 0$. Thus, Eqs. (25), (26) and (27) reduce to Eqs. (19), (20) and (21). This means that the dynamic instability occurs at the static equilibrium point

Table 1. Comparison of critical moments between static and dynamic instabilities (a=80 mm, t=1.5 mm, E=206 GP, n=0.3)

Beam length parameter/ (mm)	Critical moment (kN·m)			deflection at beam mid-section (mm)		
	Static	Dynamic	Dynamic/static	Static	Dynamic	Dynamic/static
400	33.38	23.69	0.71	7.63	10.91	1.43
500	32.95	23.39	0.71	11.76	16.70	1.42
600	32.72	23.23	0.71	16.82	24.05	1.43
700	32.58	23.13	0.71	22.84	32.89	1.44
800	32.49	23.07	0.71	29.69	42.75	1.44
900	32.43	23.03	0.71	37.52	54.40	1.45
1000	32.38	22.99	0.71	45.91	67.03	1.46
1100	32.35	22.97	0.71	55.89	81.04	1.45
1200	32.33	22.95	0.71	66.42	94.98	1.43
1300	32.31	22.94	0.71	77.88	110.59	1.42
1400	32.29	22.93	0.71	90.32	129.16	1.43
1500	32.27	22.91	0.71	102.70	148.92	1.45

of zero potential energy. Mathematically, therefore, the critical dynamic load q_{cr} and corresponding critical moment $M_{cr}=q_{cr}l^2/8$ and the constant A and flattening deformations $w_{1\max}$ and $w_{2\max}$ at the critical dynamic state can be determined by solving Eqs. (19), (20), (21) and (24). The Newtonian iteration method has also been chosen. It is worth noting the corresponding static solution can be chosen as the initial values for Newton's iteration.

Table 1 shows the result of critical dynamic moments of box-section beams of different lengths when subjected to the sudden step uniformly distributed loading. For the purpose of comparisons, the critical static moments are also superimposed in the table. It can be seen from the table that the critical dynamic moment in the sudden step load case is about 71% of the corresponding critical static moment. However, the dynamic deflection in the sudden step load case is about 1.42-1.46 of that in the corresponding static case. This finding seems to be consistent with what is reported in literature (Li *et al.*, 1997; Li, 1996; Simitses, 1987). Note that the dynamic instability discussed here is different from the bifurcation instability of dynamic systems. The analysis of dynamic instability of a structure subjected to a sudden step load requires some special treatment in numerical computations. More detailed explanation for this can be found in Simitses' book (Simitses, 1987).

5. Conclusions

The nonlinear bending responses of finite length box section beams subjected to uniformly distributed loading have been investigated. The problem has been solved analytically by modifying the Brazier approach. The nonlinear bending response related to snap-through instability of the beam has been derived analytically. The instability of the beam has been determined by using the limit-point buckling approximation for static buckling and the Simitses' method for dynamic buckling. The influence of Brazier-type nonlinearity on the critical moment has been discussed. Results have been compared with those obtained from finite element analyses, which demonstrates that the assumptions used in the present approach are rational. The results have shown that the dynamic instability of such beams occurs at a moment about 71% of the corresponding critical static moment but the dynamic deflection are almost 1.42-1.46 of those corresponding to the static instability case. The present solution can be applied to both hot-rolled and cold formed steel box-sections. However, it should be pointed out that, the nonlinear solution presented here is only for the flattening-induced nonlinearity. Other nonlinearity caused, for instance, by material yield or by large deflection of the beam is not taken into account in the present model.

References

Bedair, O. (2015). "Design expression for web shear buckling of box sections by accounting for flange restraints." *Journal of Constructional Steel Research*, 110, pp. 163-169.

Brazier, L. G. (1927). "On the flexure of thin cylindrical shells and other thin sections." *Proceedings of the Royal Society*, Series A, 116, pp. 104-114.

Hwang, W. S. Kim, Y. P. and Yoon, T. Y. (2009). "Central angle effect on connection behavior of steel box beam-to-circular column." *Structural Engineering and Mechanics*, 32(4), pp. 531-547.

Jang, G. W. Choi, S. M. and Kim, Y. Y. (2013). "Analysis of Three Thin-Walled Box Beams Connected at a Joint under Out-of-Plane Bending Loads." *Journal of Engineering Mechanics*, 139(10), pp. 1350-1361.

Kim, N. I. (2009). "Dynamic stiffness matrix of composite box beams." *Steel and Composite Structures*, 9(5), pp. 473-497.

Kim, Y. and Kim, Y. Y. (2003). "Analysis of thin-walled curved box beam under in-plane flexure." *International Journal of Solids and Structures*, 40(22), pp. 6111-6123.

Kotelko, M. Lim, T. H. and Rhodes, J. (2000). "Post-failure behaviour of box section beams under pure bending (an experimental study)." *Thin Walled Structures*, 38(2), pp. 179-194.

Lanc, D. Vo, T. P. Turkalj, G. and Lee, J. (2015). "Buckling analysis of thin-walled functionally graded sandwich box beams." *Thin Walled Structures*, 86, pp. 148-156.

Li, H. F. and Luo, Y. F. (2015). "Experimental and numerical study on cyclic behavior of eccentrically-compressed steel box columns." *Thin Walled Structures*, 96, pp. 269-285.

Li, L. Y. and Molyneaux, T. C. K. (1997). "Dynamic instability criteria for structures subjected to sudden step loads." *International Journal of Pressure Vessels and Piping*, 70(2), pp. 121-126.

Li, L. Y. (1996). "Approximate estimates of dynamic instability of long circular cylindrical shells under pure bending." *International Journal of Pressure Vessels and Piping*, 67(1), pp. 37-40.

Liu, Y. C. and Day, M. L. (2009). "Simplified modelling of thin-walled box section beam." *International Journal of Crashworthiness*, 11(3), pp. 263-272.

Liu, Y. C.(2009). "Optimum design of straight thin-walled box section beams for crashworthiness analysis." *Finite Elements in Analysis and Design*, 44(3), pp. 139-147.

Shen, H. X. (2015). "Behavior of high-strength steel welded rectangular section beam-columns with slender webs." *Thin Walled Structures*, 88, pp. 16-27.

Simitses, G. J. (1987). "Instability of dynamically-loaded structures." *Applied Mechanics Reviews*, 40(l0), pp. 1403-1408.

Vanegas, J. D. and Patino, I. D. (2013). "Linear and non-linear finite element analysis of shear-corrected composites box beams." *Latin American Journal of Solids and Structures*, 10(4), pp. 647-673.

Vo, T. P. and Lee, J. (2010). "Interaction curves for vibration and buckling of thin-walled composite box beams under axial loads and end moments." *Applied Mathematical Modelling*, 34(10), pp. 3142-3157.

Vo, T. P. and Lee, J. (2009). "Geometrically nonlinear

analysis of thin-walled composite box beams." *Computers & Structures*, 87(3-4), pp. 236-245.

Wu, Y. P. Liu, S. Z, Zhu, Y. L. and Lai, Y. M. (2003). "Matrix analysis of shear lag and shear deformation in thin-walled box beams." *Journal of Engineering Mechanics*, 129(8), pp. 944-950.

Yuan, H. X. Wang, Y. Q. Gardner L, and Shi YJ. (2015). "Local-overall interactive buckling of welded stainless steel box section compression members." *Engineering Structures*, 67, pp. 62-76.